Is an Extremely Low-Field Proton Signal in the NMR Spectrum Conclusive Evidence for a Low-Barrier Hydrogen Bond?

ARTICLE *in* THE JOURNAL OF PHYSICAL CHEMISTRY A · NOVEMBER 1997

Impact Factor: 2.69 · DOI: 10.1021/jp972335h

5 AUTHORS, INCLUDING:

Mireia Garcia-Viloca
Autonomous University of Barcelona
51 PUBLICATIONS **2,328** CITATIONS
SEE PROFILE

Angels Gonzalez-Lafont
Autonomous University of Barcelona
119 PUBLICATIONS **1,990** CITATIONS
SEE PROFILE

José M Lluch
Autonomous University of Barcelona
270 PUBLICATIONS **4,259** CITATIONS
SEE PROFILE

Is an Extremely Low-Field Proton Signal in the NMR Spectrum Conclusive Evidence for a Low-Barrier Hydrogen Bond?

Mireia Garcia-Viloca, Ricard Gelabert, Angels González-Lafont, Miquel Moreno, and José M. Lluch*

Departament de Química, Universitat Autònoma de Barcelona, 08193 Bellaterra (Barcelona), Spain

Received: July 17, 1997; In Final Form: September 8, 1997[⊗]

It has been customary to accept that the observation of a highly deshielded proton is conclusive evidence that the molecule possesses a so-called low-barrier hydrogen bond (LBHB). To analyze this point, we have theoretically studied the features of the hydrogen bonds in hydrogen maleate and hydrogen malonate anions, both compounds experimentally characterized as LBHBs, and hydrogen oxalate anion, which has a hydrogen bond of the normal type. Ab initio electronic calculations along with a monodimensional approach to solve the corresponding nuclear Schrödinger equation are combined in order to obtain the ground vibrational energy levels and wave functions associated with the proton transfer in the three systems. According to our results, in the ground vibrational state the proton connecting the hydrogen bond has a maximum probability to be found in the region of the transition state for the hydrogen maleate and hydrogen malonate systems, so that they are LBHBs, whereas for the hydrogen oxalate the proton is localized near one of the two symmetrical minimum-energy structures. Combining the chemical shifts calculated at frozen structures with the probability density functions, we have calculated the ^{1}H NMR chemical shifts for the three systems. Values of 22.85, 22.41, and 13.93 ppm for hydrogen maleate, hydrogen malonate, and hydrogen oxalate, respectively, have been obtained, results which are in good agreement with experimental values. Finally, these results allow us to discuss whether the appearance of a very high ^{1}H NMR chemical shift can be considered an unambiguous characterization of an LBHB. We postulate that an LBHB will always have an unusually downfield ^{1}H NMR chemical shift, but the opposite statement is not necessarily true.

Introduction

Hydrogen bonds play an important role in many ways in chemistry and biochemistry. In particular, it is widely recognized that hydrogen bonds can stabilize transition states in enzyme mechanisms, this way decisively contributing to the enormous catalytic power of enzymes.[1−3] A special class of hydrogen bonds, the so-called low-barrier hydrogen bonds (LBHBs),[4] have recently been proposed as a major factor in enzyme catalysis.[5−12] According to some authors,[7,8] formation of such a bond would supply 10−20 kcal/mol, in this way facilitating otherwise very difficult reactions. This suggestion has provoked opposing viewpoints leading to an intense debate on the strength of an LBHB and its function in enzymic catalysis.[2,3,13−18]

Although interest in LBHBs has revived because of their possible catalytic relevance in sizable biological systems, some of their intrinsic properties still remain unclear, even in chemical systems in solution or in the gas phase, and considerable effort is being devoted to study them.[13−23] Some authors claim that, for LBHB to have a conceptual existence separate from that of an ordinary hydrogen bond, its nature should be different. That is, the relative weights of its "electrostatic" and "covalent" components ought to be significantly different from those in an ordinary hydrogen bond.[3] Given that depending on which property is considered different definitions of an LBHB could be given, we have adopted an operational definition that does not go beyond what is already implied in the name "low-barrier hydrogen bond". In a hydrogen bond the proton is shared by two electronegative atoms, and the potential energy hypersurface associated with its motion from one to the other is a multidimensional double well. That is, the two minimum-energy structures, each one corresponding to the proton attached to one or the other of the electronegative atoms, are separated by a classical energy barrier, i.e., without including zero-point energy.[11] We assume that if the classical energy barrier is low enough so that the nuclear wave function corresponding to the ground vibrational level of the double well reaches its maximum values at the region of that energy barrier, then this hydrogen bond can be considered an LBHB. In a monodimensional approach corresponding to the double-well reaction path describing the proton jump that condition is fulfilled provided that the ground vibrational level of the monodimensional double-well lies at or above the classical energy barrier. As a matter of fact, there is no sharp differentiation between hydrogen bonds whose lowest vibrational level is just above the barrier and those just below the barrier.[24] A very particular kind of LBHB would appear if the classical energy barrier were nul, in which case a single-well hydrogen bond would result.

Taking into account the above definition, the best physical characterization of an LBHB is the measurement of the proton location by neutron-diffraction studies: if the proton is found to be near the midpoint between the heavier atoms, the hydrogen bond turns out to be an LBHB. Some alternative and easier-to-measure physicochemical parameters to identify LBHBs have been proposed. In particular, the appearance of an unusually downfield nuclear magnetic resonance (NMR) chemical shift δ for the participating proton, within the range from 16 to 20 parts per million (ppm), has been considered as the most unambiguous of them.[8] However, very recently, Warshel and Papazyan[3] and Guthrie[2] have claimed that interpreting large chemical shifts as unambiguous LBHB indicators is fundamentally flawed.

The purpose of this paper is to discuss whether the observation of a highly deshielded proton is really conclusive evidence

[⊗] Abstract published in *Advance ACS Abstracts,* October 15, 1997.

S1089-5639(97)02335-9 CCC: $14.00

for an LBHB. To this aim, we have theoretically studied the features of the hydrogen bonds in hydrogen maleate and hydrogen malonate. Both compounds are supposed to contain an LBHB because the acidic proton in the tetrabutylammonium salts of hydrogen maleate and hydrogen 2,2-dimethylmalonate exhibit ^{1}H NMR chemical shifts of 19.5−20.3 ppm in several organic solvents, the values corresponding to the hydrogen maleate being somewhat higher than the ones associated with hydrogen 2,2-dimethylmalonate.[8]

Calculational Details

Ab initio restricted Hartree−Fock calculations have been carried out using the split-valence 6-31+G(d,p) basis set, which includes d and p polarization functions on heavy and hydrogen atoms, respectively, and a diffuse sp shell on heavy atoms.[25] Correlation energy has been included by means of the second-order Møller−Plesset perturbation theory.[26,27] Full geometry optimization and direct localization of stationary points have been done with the Schlegel gradient optimization algorithm[28] at the MP2 level of calculation. The characterization of both kinds of stationary points, minima or transition-state structures, has been carried out by diagonalizing their Hessian matrixes and looking for zero or one negative eigenvalues, respectively. We have to emphasize that the obtention of the MP2 frequencies for these systems requires up to 6 GB of disk usage, what indicates the high computational cost of the calculations.

^{1}H NMR chemical shifts (δ) relative to hydrogen atoms in $Si(CH_3)_4$ have been obtained from nuclear magnetic shielding tensors calculated through the GIAO[29,30] (gauge invariant atomic orbital) method. The GIAO chemical shifts have been calculated using the Hartree−Fock wave functions. As known, correlation effects are often generally important in NMR shielding calculations of heavy atoms.[31] However, it has been recognized that correlation effects on hydrogen shielding constants can be relatively small (of the order of 0.1−0.3 ppm, with the exception of molecules involving fluorine).[31] All electronic structure calculations have been done with the GAUSSIAN 94 package.[32]

We are interested in the evaluation of the values of the chemical shifts of transferring protons, corresponding to a given vibrational state rather than to a frozen arrangement of nuclei (that is, a fixed molecular geometry). Concretely, this implies evaluating averaged δ values using $|\psi|^2$, the square of the vibrational wave function, as a weighting factor. Consequently, we have to obtain the vibrational eigenvalues and eigenfunctions. To do so, the nuclear motion Schrödinger equation has to be solved:

$$[\hat{T}_{\text{nuc}} + U(\mathbf{R})]\Psi = E\Psi \tag{1}$$

where $U(\mathbf{R})$ is the complete potential energy hypersurface, which depends on $\mathbf{R}$, a $3N - 6$ element vector that describes each different geometrical arrangement of the atoms of the molecule. Of course, calculating the whole $U(\mathbf{R})$ is impossible except for the simplest of all systems, so a drastic simplification is needed. The most straightforward simplification consists of reducing the dimensionality of $U(\mathbf{R})$ to just one dimension. In this way, both the evaluation of U and solving eq 1 become feasible tasks for sizable systems. The problem is the choice of the variable on which U depends. Given that any monodimensional path is just as good as any other, provided it represents the chemical process under study (in our case, an intramolecular proton transfer within the corresponding hydrogen bond), we have opted for a linear interpolation in mass-weighted Cartesian coordinates linking the transition-state structure with the reactants' structure, and then we extrapolate beyond that point farther from reactants and opt for yet another linear interpolation in the same coordinate system going from the transition-state structure to the products' minimum and the corresponding extrapolation beyond. These linear paths have been constructed orientating both structures involved in such a way that neither linear nor angular momenta were generated when going from one to the other.[33] After the number of variables of U has been reduced in this way to just one, a basis set methodology has been used to solve eq 1.[34] Within this methodology, the vibrational energy levels and wave functions are obtained through diagonalization of the matrix representation of the Hamiltonian operator in (1) projected over a basis set made up of monodimensional Gaussian functions:

$$\chi_i(s) = \left(\frac{\alpha}{\pi}\right)^{1/4} \exp\left(-\frac{\alpha}{2}(s - s_i)^2\right) \tag{2}$$

In eq 2 s is the arc distance along the reaction path in mass-weighted Cartesian coordinates and $\{s_i\}$ are equally spaced points along the aforementioned linear path. In this way n variational approximations to the lowest n eigenvalues and eigenfunctions can be obtained by using n basis functions. In this work, different numbers of basis functions have been used in the different cases, so that the density of Gaussian functions was approximately the same in all systems studied. It was checked that a further increase in the number of basis functions did not noticeably change the position of the vibrational levels.

The vibrational wave function obtained in this way is expressed as a linear combination of basis functions. To take into account the motion of the nuclei in a vibrational state, values of δ of the proton have been evaluated at several points along the path (values of s) and then fitted into a cubic spline functional form. Finally, the mean value of δ is obtained as an average all over the vibrational states taking into account the appropriate probability density function, in this case $|\psi|^2$, by means of

$$\langle\delta\rangle = \frac{\int_{-\infty}^{+\infty}\Psi(s)\,\delta(s)\,\Psi(s)\,\mathrm{d}s}{\int_{-\infty}^{+\infty}\Psi(s)\,\Psi(s)\,\mathrm{d}s} \tag{3}$$

Chemical shift (δ) values corresponding to frozen geometries of nuclei (when calculated in ppm) are mass-independent, that is, do not change with the isotopic composition of the system. However, averaged δ values (see eq 3) must change when the hydrogen-bonding proton is substituted by deuterium because probability density functions $|\psi|^2$ are different for each isotope. For that reason, $<\delta>$ values have been calculated for both H and D, building up the adequate linear path in mass-weighted Cartesian coordinates in each case.

Results and Discussion

Even though our interest is centered on the hydrogen maleate and hydrogen malonate systems, for these are allegedly LBHB; we will include a third system in our study for the sake of completeness. This additional system is hydrogen oxalate. This system has an intramolecular hydrogen bond of the normal type. In this way, we will have data regarding systems with intramolecular hydrogen bonds, in which the proton transfer takes place in rings made up of 7 (hydrogen maleate, **1**), 6 (hydrogen malonate, **2**), and 5 (hydrogen oxalate, **3**) atoms.

First, stationary points were sought for the three systems, and they were characterized by means of Hessian evaluation and diagonalization. Table 1 shows some interesting geometrical

TABLE 1: Most Interesting Geometrical Parameters of the Stationary Points, along with the Classical Potential Energy Barrier of the Intramolecular Proton Transfer[a]

	O_1-H	$H-O_2$	$O_1\cdots O_2$	$\Delta V^{\ddagger}$
1 R	1.12	1.30	2.41	
1 TS	1.20	1.20	2.40	0.03
2 R	1.09	1.37	2.43	
2 TS	1.21	1.21	2.39	0.17
3 R	1.00	1.71	2.50	
3 TS	1.22	1.22	2.33	3.12

[a] Distances and energies are given in Å and kcal/mol, respectively. Numbers **1**, **2,** and **3** refer to the corresponding structures in Figure 1. R and TS stand for reactant and transition state for each intramolecular proton transfer.

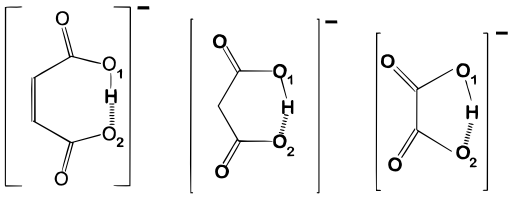

Figure 1. Schematic representation of the systems studied in this work.

parameters of these stationary points, along with the classical potential energy barrier of the intramolecular proton transfer in the rightmost column in the same table.

Even though systems **1**, **2,** and **3** bear some similarities, it has to be noted that there are some differences worth mentioning. To begin with, systems **1** and **3** are planar, while system **2** is not. With respect to potential energy barriers of the corresponding proton transfer, it can be seen that the higher the number of atoms in the cyclic structure in which the proton transfer takes place, the lower the potential energy barrier becomes. Moreover, it can also be seen that when the energy barrier of the proton transfer is small, the distance between the transferring proton and the donor oxygen atom becomes longer. This behavior is simultaneous with a shortening of the distance between the proton and the acceptor oxygen atom. In other words, focusing on the O_1-H, $H\cdots O_2$, and $O_1\cdots O_2$ distances, it can be seen that the geometries of the transition-state structure and of the minimum become more and more alike when the potential energy barrier decreases. The foreseeable limit of this trend would be a hydrogen bond in which the proton is halfway between both oxygen atoms. In such a case, the proton transfer would have, obviously, no potential energy barrier.

Let us turn our attention to the ^1H NMR chemical shift corresponding to the transferring proton. The δ values for the stationary points of the three systems presented in Figure 1 are given in the first column of Table 2. These values are calculated relative to tetramethylsilane (TMS) by means of

$$\delta = \sigma_{TMS} - \sigma \tag{4}$$

where σ is the shielding constant. At our level of calculation $\sigma_{TMS} = 32.15$ ppm. As for the reactants it can be seen that δ decreases as the ring size diminishes (that is, from **1** to **3**). On the other hand, for a given system, δ is somewhat greater (quite greater for the hydrogen oxalate) at the transition state than at the reactant. To analyze these facts, we have separated the shielding constant in terms of its diamagnetic, σ_d, and paramagnetic, σ_p, contributions (second and third column in Table 2):

$$\sigma = \sigma_d + \sigma_p \tag{5}$$

TABLE 2: NMR Chemical Shifts, Diamagnetic and Paramagnetic Contributions to the Shielding Constants, and Anisotropies Corresponding to the Studied Structures (All Values in ppm)[a]

	δ	σ_d	σ_p	$\Delta\sigma$
1 R	23.19	18.25	−9.29	36.05
1 TS	24.38	17.12	−9.35	37.51
2 R	21.39	18.31	−7.55	31.85
2 TS	23.96	15.98	−7.79	35.24
3 R	13.39	26.06	−7.30	18.57
3 TS	23.51	17.20	−8.56	33.99
4 T1	5.49	29.31	−2.65	11.65
4 T2	8.70	25.05	−1.60	9.37
4 T3	9.82	23.75	−1.42	8.49
4 T4	10.86	22.67	−1.38	7.68

[a] Numbers **1**, **2**, and **3** refer to the corresponding structures in Figure 1. R and TS stand for reactant and transition state for each intramolecular proton transfer. **4** stands for the trans isomer of structure **1**, with different O_1-H values: 0.97 (minimum-energy trans structure), 1.09, 1.14, and 1.19 Å being denoted by T1, T2, T3, and T4, respectively.

In previous works it has been shown the dominant influence of the proton acceptor and donor atoms on the proton shielding constant. Proton shielding in the $O_1-H\cdots O_2$ hydrogen bond is reduced with increasing O_1-H distance and also with decreasing $O_1\cdots O_2$ distance (or rather the $H\cdots O_2$ distance).[1,35,36] The diamagnetic and paramagnetic contributions are respectively mainly responsible for these two effects. In effect, from inspection of both Tables 1 and 2 it can be seen that the three reactants follow these trends. Besides, in going from each reactant to the corresponding transition state, the increase of the O_1-H distance and the decrease of the $H\cdots O_2$ distance cause respectively the diminution of both σ_d and σ_p, in such a way that the deshielding effect increases. On the other hand, these simple rules are not sufficient to correlate the values associated with the three transition states. For this purpose it would be probably necessary to consider the variation of the $O_1-H\cdots O_2$ angle at each transition state, which is almost 180° in hydrogen maleate but only 145° in hydrogen oxalate. In addition, it has to be recalled that systems **1** and **3** are planar, but **2** is not.

If the hydrogen bond is broken, as seen by comparison of cis and trans hydrogen maleate in Table 2, both σ_d and σ_p clearly grow, in such a way that the chemical shift moves upfield. For the trans structure it is clear that only the O_1-H distance is relevant, its increase provoking a proton deshielding. On the other hand, it has been proposed that anisotropy, $\Delta\sigma$, may be a more sensitive measure of the degree of hydrogen bonding than the isotropic σ value.[35] As a matter of fact, a shielding tensor can be characterized by both the anisotropy

$$\Delta\sigma = \sigma_{33} - {}^1/_2(\sigma_{11} + \sigma_{22}) \tag{6}$$

and the isotropic shielding

$$\sigma = {}^1/_3(\sigma_{11} + \sigma_{22} + \sigma_{33}) \tag{7}$$

where the diagonal values in the diagonalized shielding tensor, σ_{11}, σ_{22}, and σ_{33}, are ordered such that $\sigma_{11} > \sigma_{22} > \sigma_{33}$. So, loss of a hydrogen bond in trans hydrogen maleate implies a noticeable decrease of the anisotropy (see last column in Table 2).

From the results obtained up to here we can deduce that, in general, transition states for proton-transfer reactions will give a very low-field proton signal (very high δ values) because the jumping proton lies at the midpoint region between both heavy atoms (large O_1-H distance, but relatively short $H\cdots O_2$ distance, especially taking into account that the $O_1\cdots O_2$ distance tends

TABLE 3: Path Length from Reactant to Product, Classical Potential Energy Barrier, and Energy of the First Vibrational State for Each Intramolecular Proton Transfer; Energies Are Relative to the Minimum-Energy Structures

	Δs^a	$\Delta V^{\ddagger b}$	ΔE^b
1	0.285	0.03	0.64
2	0.713	0.17	0.32
3	1.418	3.12	0.97

[a] In amu$^{1/2}$ Å. [b] In kcal/mol.

to be reduced in going from the reactants to the transition state). The scenario for the reactants is different. If the $O_1\cdots O_2$ distance is long, the reactants will exhibit normal δ values. Instead, if the $O_1\cdots O_2$ distance is short enough, the O_1-H distance tends to be large and the $H\cdots O_2$ distance short, leading to quite deshielded protons (with high or even very high δ values).

At this point it has to be recalled that neither the δ values at the reactants nor those at the transition states correspond directly to what is experimentally found for the systems shown in Figure 1. δ values displayed in Table 2 are associated with particular frozen positions of the proton. However, the quantum nature of the hydrogen atoms (intrinsically associated with their vibrational wave function) causes their delocalization along the hydrogen bond (just in the same sense as the electrons are delocalized according to their electronic wave functions). The chemical shifts that are experimentally measured arise from the average of the δ values at all the positions in the hydrogen bond, taking into account the probability density derived from the delocalization. Then, as explained above, we have calculated averages of δ values weighted by the probability density of the one-dimensional vibrational functions. As a matter of fact, we have only used the ground-state vibrational wave function, in such a way that the mean values would correspond to the chemical shift at 0 K. Determination of $\langle\delta\rangle$ at higher temperatures would require the calculation of higher vibrational levels and their thermal population.

According to the general procedure outlined in the calculational details section, we have chosen a path consisting of two linear segments as the proton-transfer reaction path. Due to the fact that these paths have been evaluated in mass-weighted Cartesian coordinates, they are dependent on the isotopic composition of the system and hence must be rebuilt for each isotopomer of the system we want to study. Then, for each system the potential energy and the δ values were calculated at several points along the corresponding proton-transfer reaction path. Both magnitudes were fitted into cubic splines functional forms. In this way a potential energy profile $U(s)$, and a function describing $\delta(s)$ were obtained. The vibrational energy levels were calculated, then, following the methodology set forth in the calculational details section. The details and some results of these calculations are presented in Table 3.

Several interesting points can be highlighted from Table 3. To begin with, and in accord with the conclusions relative to the geometry of the minimum-energy structures of systems **1**−**3** discussed previously, the distance between minima in mass-weighted Cartesian coordinates decreases along with the potential energy barrier of the corresponding proton transfer. However, more interesting details come from the values of the zero-point energy levels. As expected, for the case of hydrogen oxalate (**3**) the first vibrational level appears well below the classical potential energy barrier. It must be said that this energy level is the first of a pair of levels very close in energy, which appear due to the coupling of two degenerate states localized in each of the wells when the potential energy barrier is infinite in height. As for hydrogen maleate and hydrogen malonate (**1** and **2**, respectively), the first vibrational energy level appears above the classical potential energy barrier of the proton transfer. This fact alone within our monodimensional approach allows us to classify as LBHB the cases of hydrogen maleate and hydrogen malonate, while the case of hydrogen oxalate corresponds to a normal hydrogen bond.

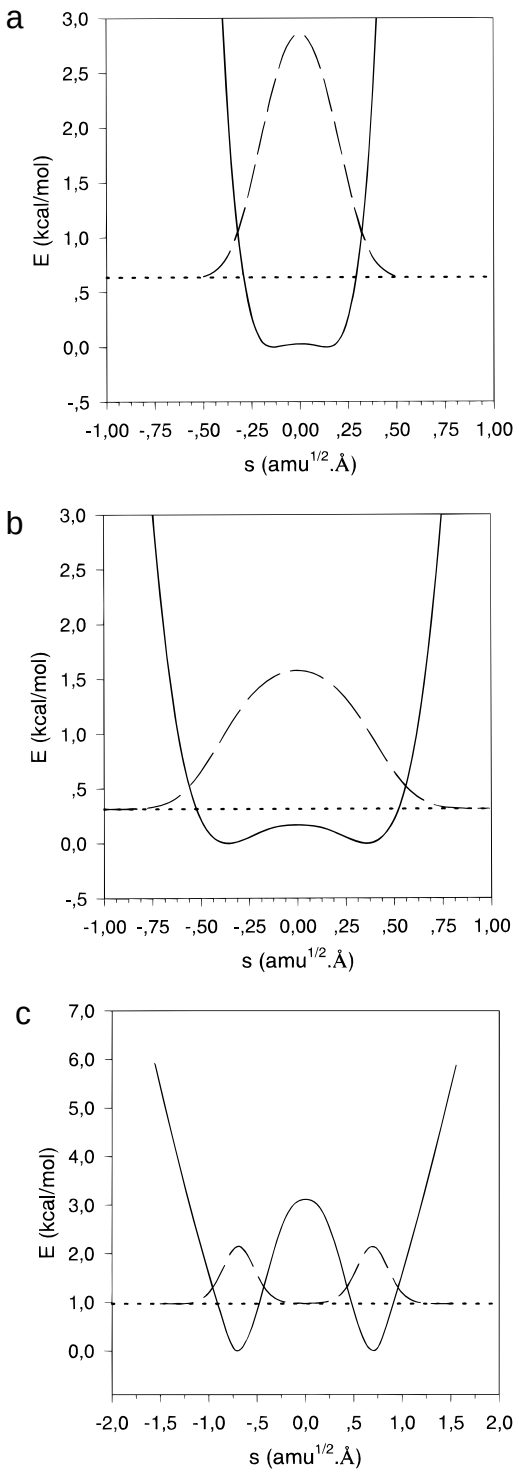

Figure 2. Monodimensional energy profile as a function of s for the three intramolecular proton transfers (solid line) and their corresponding first vibrational levels (dotted line) and probability density functions (dashed line): (a) hydrogen maleate, (b) hydrogen malonate, and (c) hydrogen oxalate.

The consequences of the position in energy of the first vibrational level of these systems will be better understood by examining the probability density function of these states, $|\psi|^2$, which is depicted for the three systems in Figure 2.

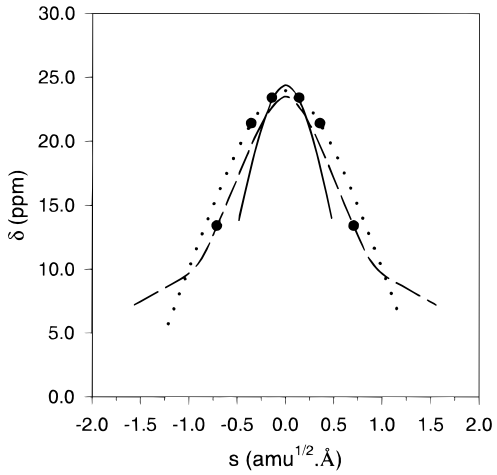

Figure 3. Proton NMR chemical shift along the reaction paths. Marks (●) indicate the location corresponding to the minimum-energy structures in each case: hydrogen maleate (solid line), hydrogen malonate (dotted line), and hydrogen oxalate (dashed line).

As can be seen in Figure 2, both hydrogen maleate and hydrogen malonate, having their first vibrational level above the classical potential energy barrier of the proton transfer, possess a probability density function that is inherently different from that of hydrogen oxalate. In the latter case the wave function has a greater amplitude just over both minima, whereas in the case of hydrogen malonate and hydrogen maleate the greatest amplitude of the wave function appears precisely over the region of the transition-state structure of the proton transfer. What are the consequences of this difference? In the case of the hydrogen oxalate, the proton can be said to be "localized" in the neighborhood of one oxygen—either the donor or the acceptor. On the other hand, in the cases of hydrogen maleate and hydrogen malonate the proton will most probably be found in the region of the transition state. This fact will have interesting consequences in relation to the behavior of these systems. That is, some global properties of the systems can resemble those of the transition-state structure rather than those of the minima.

As for the proton chemical shift, the $\delta(s)$ functions along the reaction paths corresponding to hydrogen maleate, hydrogen malonate, and hydrogen oxalate are displayed in Figure 3. Negative or positive s values stand respectively for the region before or after the transition state, for which the value is assigned. The three curves are qualitatively analogous. For each curve, the δ value has a maximum at the transition state and goes down monotonically toward the minimum-energy structure. The fact that the three molecules are symmetrical with respect to the intramolecular proton transfer should be recalled. The larger the path between the transition state and the minimum (and, therefore, the more separated both equivalent minima), the greater the δ fall is. Beyond the minimum, the proton is pushed toward the heavy atom to which it is bonded, in such a way that the shielding constant increases (mainly as a consequence of its diamagnetic component) and the chemical shift decreases still more.

Combining the curves in Figure 3 with probability density functions shown in Figure 2, we have obtained 22.85, 22.41, and 13.93 ppm as $\langle\delta\rangle$ values for hydrogen maleate, hydrogen malonate, and hydrogen oxalate, respectively.

For hydrogen maleate $\langle\delta\rangle$ turns out to be smaller than not only the δ value of the transition state but also the δ value of the minima. This is because such a short hydrogen bond (small separation between both minima) has an important fraction of the probability density in the zone where δ reaches the lower values, that is, outside the region between the two minima. Conversely, in hydrogen malonate, with a longer hydrogen bond, the weight of the vibrational wave function further away from the minima ($|s| > 0.36$ amu$^{1/2}$ Å) is small, in such a way that $\langle\delta\rangle$ is near the midpoint between the chemical shifts corresponding to the minima and the transition state. Finally, the vibrational wave function in hydrogen oxalate has no important contribution at the transition-state region, in such a way that $\langle\delta\rangle$ only slightly surpasses the δ value of the minima.

The $\langle\delta\rangle$ values calculated in this work for the three systems studied are in quite good agreement with the reported experimental results. In particular, Frey et al.[8] measured in three different organic solvents chemical shifts that range from 19.5 to 19.6 ppm and from 20.2 to 20.3 ppm for the tetrabutylammonium salts of hydrogen maleate and hydrogen malonate, respectively. Although the theoretical $\langle\delta\rangle$ values are both somewhat overestimated, the experimental difference between both compounds is quite well reproduced by our theoretical calculations. For ammonium hydrogen oxalate hemihydrate, values of 14.0 and 15.6 ppm have been measured by NMR spectroscopy in the solid state.[37,38]

Another physicochemical parameter that has been used to characterize LBHBs is the isotope effect on the chemical shift[1,39] when the protium forming the hydrogen bond is substituted by a deuterium:

$$\Delta = \langle\delta(^1\mathrm{H})\rangle - \langle\delta(^2\mathrm{H})\rangle \qquad (8)$$

So, it has been predicted that for normal hydrogen bonds Δ will have a value close to zero or a positive value depending on whether the minima are quite deep with a low anharmonicity or the central energy barrier is low, introducing a significant anharmonicity. Conversely, an LBHB would be associated with a negative value of Δ. Concretely, $\Delta = -0.03$ ppm has been experimentally measured for the hydrogen maleate anion.[1,39] In good agreement with those predictions, our calculations provide Δ values of -0.16, -0.02, and 0.1 ppm for hydrogen maleate, hydrogen malonate, and hydrogen oxalate, respectively. The effect of the isotopic substitution is somewhat greater for **1** than for **2**, probably due to the fact that the contribution of the hydrogen atom to the total motion of the molecule along the intramolecular proton transfer reaction path is bigger for hydrogen maleate. So, when protium is substituted by deuterium, the reaction path length only increases 8% in mass-weighted Cartesian coordinates for hydrogen malonate, whereas it augments 20% for hydrogen maleate. We have to note that we are handling very low values of Δ, both from the theoretical and the experimental points of view, which casts some doubts about their accuracy. Anyway, our results confirm the expected trends of Δ, attributing its negative values for **1** and **2** (two LBHBs) to the higher vibrational amplitudes of the light atoms (as a consequence of the more spread vibrational wave function). As can be seen in Figure 3, the more important the weight of the region far from the proton-transfer transition state, the lower the chemical shift, leading to negative Δ values for the LBHBs in **1** and **2**.

Conclusions

In this paper we have obtained the ground vibrational energy levels and wave functions associated with the proton jump between the two oxygen atoms in the intramolecular hydrogen bonds involved in hydrogen maleate, hydrogen malonate, and hydrogen oxalate in the gas phase. To this aim, we have used ab initio electronic calculations along with a monodimensional approach to solve the corresponding nuclear Schrödinger

equation. According to our results, the ground vibrational wave function reaches its maximum value at the region of the intramolecular-proton-transfer transition state for hydrogen maleate and hydrogen malonate. Therefore, in these two systems the proton connecting the hydrogen bond will most probably be found in the region of the transition state. In other words, hydrogen bonds in both hydrogen maleate and hydrogen malonate are identified as low-barrier hydrogen bonds (LBHBs). Conversely, hydrogen oxalate contains a normal hydrogen bond, in which the proton is localized in the neighborhood of one oxygen, either the donor or the acceptor. At this point, it should be noted that, at least in the gas phase, the schematic frozen structures displayed in Figure 1 do not correctly reproduce the true proton location of the real systems. That is, for hydrogen maleate and hydrogen malonate, which contain an LBHB, the proton is fully delocalized along the hydrogen bond, the maximum of its probability density function corresponding to the transition-state region. Then, a pictorial representation like $O_1 \cdots H \cdots O_2$ would be more appropiate than $O_1-H \cdots O_2$. The scenario is somewhat different for hydrogen oxalate. In this case $O_1-H \cdots O_2$ would indicate the existence of a proton located near a given oxygen atom. However, this situation does not correspond to a stationary state of the double-well system. Instead, a picture like $O_1-H \cdots O_2 \leftrightarrow O_1 \cdots H-O_2$, indicating a coupling between two zero-order nuclear wave functions, would be better.

On the other hand, combining the chemical shifts calculated at frozen structures with the corresponding probability density functions, we have obtained the ^{1}H NMR chemical shifts for the three systems studied in this work. Values of 22.85, 22.41, and 13.93 ppm for hydrogen maleate, hydrogen malonate, and hydrogen oxalate, respectively, have been obtained. Although the two first theoretical values are somewhat overestimated, the experimental difference between them is quite well reproduced, and hydrogen oxalate's theoretical $\langle\delta\rangle$ is also comparable to experimental measurements.

Let us now try to answer the main question raised at the beginning of the present paper: what is the specific relationship between the existence of an LBHB and the appearance of a particular ^{1}H NMR chemical shift value associated with the hydrogen-bonded atom? From the above results we can infer that, of the three systems studied, the two classified as LBHBs (hydrogen maleate and hydrogen malonate) have unusually downfield chemical shifts, while hydrogen oxalate, with a normal hydrogen bond, presents a much lower $\langle\delta\rangle$ value. Hence, one could draw from our calculations that a deshielded proton in a hydrogen bond with a remarkably high chemical shift is conclusive evidence of an LBHB, in good accord with the already mentioned opinion of several authors who have used δ measurements in the range 16−20 ppm as an unambiguous characterization of an LBHB.[17] Let us, however, analyze the different aspects of the problem in more detail.

Our study of the ground vibrational energy levels and probability density functions associated with the proton transfer in the three intramolecular gas-phase hydrogen-bonded systems analyzed has clearly revealed that in an LBHB the proton will most likely be found in the region of the transition state. In this region the proton is highly deshielded because the proton has moved away from the donor oxygen atom (large O_1-H distances) with the corresponding decrease in σ_d, but at the same time, it has approached the acceptor oxygen atom (short $H \cdots O_2$ distances) which provokes a decrease of σ_p. The diminution of the two contributions to the proton total shielding constant at the transition state midpoint region explains the high values found for $\langle\delta\rangle$ in hydrogen maleate and hydrogen malonate. It hence seems clear that there is a class of hydrogen bonds called LBHBs that show remarkably high ^{1}H NMR chemical shifts. However, we should not expect that the reverse of the same statement is always valid. That is, any system with an unusually downfield ^{1}H NMR chemical shift does not necessarily have an LBHB, even though it is a first indication, if not a conclusive one, that an LBHB could exist in the chemical system.

Normal hydrogen bonds, which have ground vibrational probability density functions with two maxima, one at the donor atom region and the other at the acceptor atom region, can also present unusually high ^{1}H NMR chemical shifts. To illustrate this point, let us refer again to hydrogen maleate and hydrogen malonate cases. The function describing $\delta(s)$ reveals that in the two LBHBs studied in this work δ is already high at the minimum-energy structures (in particular, it takes values of 23.2 and 21.4 ppm for hydrogen maleate and hydrogen malonate, respectively), although $\delta(s)$ reaches a maximum at the transition state. This means that, without invoking LBHB formation, minimum-energy hydrogen-bonded structures with the transferring proton attached to either the donor or the acceptor atom (short O_1-H or short $H-O_2$ distances, respectively) can already show ^{1}H NMR chemical shifts in the range 16−20 ppm or higher. Our main conclusion on this point is that an unusually downfield chemical shift does not necessarily imply the formation of an LBHB. The only cases where high average ^{1}H NMR chemical shifts may only be explained as a direct consequence of LBHB formation are those systems with upfield chemical shifts at the minimum-energy structures of the proton-transfer process along the hydrogen bond. Thus, the only way that the average chemical shift for those systems may turn out to be in the high range depends on the formation of an LBHB because, as we have already seen, the maximum probability of finding the proton in an LBHB appears at the most deshielded region, that of the transition state.

Our opinion is that the only requirement of a hydrogen bond in order to be characterized by a high ^{1}H NMR chemical shift is that it must be short at the minimum-energy structures. Then, the short hydrogen acceptor interaction weakens the donor hydrogen bond, and the proton total shielding constant decreases. A short donor−acceptor distance is also a requirement for LBHB formation. That explains why those two features (high chemical shifts and LBHB character) may usually come together although the delocalization of an LBHB will not always be the cause of that distinctive NMR spectra of the transferring proton. A globally neutral hydrogen bond is an interesting example. Let us assume that the two minima of the double well are nondegenerate, in such a way that the well corresponding to $A^- \cdots H - B^+$ is lower than the $A-H \cdots B$ one. Then, the classical energy barrier relative to the ionic minimum may be high (as a result of adding the absolute value of the energy difference between both minima to the energy barrier relative to the upper well), so leading to a normal hydrogen bond in which the shifting proton will be attached to the B heavy atom. However, this localized ionic complex will involve a very short hydrogen bond with a highly deshielded proton, this way leading to a very large proton chemical shift.[23]

Acknowledgment. Financial support from DGES through Project No. PB95-0637 and the use of the computational facilities of the "Centre de Computació i de Comunicacions de Catalunya" are gratefully acknowledged.

References and Notes

(1) Hibbert, F.; Emsley, J. *Adv. Phys. Org. Chem.* **1990**, *26*, 255.
(2) Guthrie, J. P. *Chem. Biol.* **1996**, *3*, 164.

(3) Warshel, A.; Papazyan, A. *Proc. Natl. Acad. Sci. U.S.A.* **1996**, *93*, 13665.
(4) Cleland, W. W. *Biochemistry* **1992**, *31*, 317.
(5) Gerlt, J. A.; Gassman, P. G. *J. Am. Chem. Soc.* **1993**, *115*, 11552.
(6) Gerlt, J. A.; Gassman, P. G. *Biochemistry* **1993**, *32*, 11943.
(7) Cleland, W. W.; Kreevoy, M. M. *Science* **1994**, *264*, 1887.
(8) Frey, P. A.; Whitt, S. A.; Tobin**,** J. B. *Science* **1994**, *264*, 1927.
(9) Kenyon, G. L.; Gerlt, J. A.; Petsko, G. A.; Kozarich, J. W. *Acc. Chem. Res.* **1995**, *28*, 178.
(10) Xiang, S.; Short, S. A.; Wolfenden, R.; Carter, C. W. *Biochemistry* **1995**, *34*, 4516.
(11) Cleland, W. W.; Kreevoy, M. M. *Science* **1995**, *269*, 104.
(12) Frey, P. A. *Science* **1995**, *269*, 104.
(13) Warshel, A.; Papazyan, A.; Kollman, P. A. *Science* **1995**, *269*, 102.
(14) Schwartz, B.; Drueckhammer, D. G. *J. Am. Chem. Soc.* **1995**, *117*, 11902.
(15) Alagona, G.; Ghio, C.; Kollman, P. A. *J. Am. Chem. Soc.* **1995**, *117*, 9855.
(16) Scheiner, S.; Kar, T. *J. Am. Chem. Soc.* **1995**, *117*, 6970.
(17) Tobin, J. B.; Whitt, S. A.; Cassidy, C. S.; Frey, P. A. *Biochemistry* **1995**, *34*, 6919.
(18) Shan, S.-O.; Herschlag, D. *Proc. Natl. Acad. Sci. U.S.A.* **1996**, *93*, 14474.
(19) Smirnov, S. N.; Golubev, N. S.; Denisov, G. S.; Benedict, H.; Schah-Mohammedi, P.; Limbach, H.-H. *J. Am. Chem. Soc.* **1996**, *118*, 4094.
(20) Huskey, W. P. *J. Am. Chem. Soc.* **1996**, *118*, 1663.
(21) Cassidy, C. S.; Lin, J.; Frey, P. A. *Biochemistry* **1997**, *36*, 4576.
(22) Garcia-Viloca, M.; González-Lafont, A.; Lluch, J. M. *J. Am. Chem. Soc.* **1997**, *119*, 1081.
(23) Garcia-Viloca, M.; González-Lafont, A.; Lluch, J. M. *J. Phys. Chem.* **1997**, *101*, 3880.
(24) Kreevoy, M. M.; Liang, T. M. *J. Am. Chem. Soc.* **1980**, *102*, 3315.
(25) (a) Clark, T.; Chandrasekhar, J.; Spitznagel, G. W.; Schleyer, P. v. R. *J. Comput. Chem.* **1983**, *4*, 294. (b) Frisch, M. J.; Pople, J. A.; Binkley, J. S. *J. Chem. Phys.* **1984**, *80*, 3265.
(26) Møller, C.; Plesset, M. S. *Phys. Rev.* **1934**, *46*, 618.
(27) Binkley, J. S.; Pople, J. A. *Int. J. Quantum Chem.* **1975**, *9*, 229.
(28) Schlegel, H. B *J. Comput. Chem.* **1982**, *3*, 214.
(29) Ditchfield, R. *Mol. Phys.* **1974**, *27*, 789.
(30) Wolinski, K.; Hinton, J. P.; Pulay, P. *J. Am. Chem. Soc.* **1990**, *112*, 8251.
(31) Chesnut, D. B. *Chem. Phys.* **1997**, *214*, 73.
(32) Frisch, M. J.; Trucks, G. W.; Schlegel, H. B.; Gill, P. M. W.; Johnson, B. G.; Robb, M. A.; Cheeseman, J. R.; Keith, T. A.; Petersson, G. A.; Montgomery, J. A.; Raghavachari, K.; Al-Laham, M. A.; Zakrzewski, V. G.; Ortiz, J. V.; Foresman, J. B.; Cioslowski, J.; Stefanov, B. B.; Nanayakkara, A.; Challacombe, M.; Peng, C. Y.; Ayala, P. Y.; Chen, W.; Wong, M. W.; Andres, J. L.; Replogle, E. S.; Gomperts, R.; Martin, R. L.; Fox, D. J.; Binkley, J. S.; Defrees, D. J.; Baker, J.; Stewart, J. P.; Head-Gordon, M.; Gonzalez, C.; Pople, J. A. *Gaussian94*; Gaussian, Inc.: Pittsburgh, PA, 1995.
(33) Miller, W. H.; Ruf, B. A.; Chang, Y. *J. Chem. Phys.* **1988**, *89*, 6298.
(34) (a) Hamilton, I. P.; Light, J. *J. Chem. Phys.* **1986**, *84*, 306. (b) Makri, N.; Miller, W. H. *J. Chem. Phys.* **1987,** *86*, 1451.
(35) Ditchfield, R. *J. Chem. Phys.* **1976**, *65*, 3123.
(36) Berglund, B.; Vanghan, R. W. *J. Chem. Phys.* **1980**, *73*, 2037.
(37) Jeffrey, G. A.; Yeon, Y. *Acta Crystallogr.* **1986**, *B42*, 410.
(38) Zheng, L.; Fishbein, K. W.; Griffin, R. G.; Herzfeld, J. *J. Am. Chem. Soc.* **1993**, *115*, 6254.
(39) Altman, L. J.; Laungani, D.; Gunnarsson, G.; Wennerström, H.; Forsén, S. *J. Am. Chem. Soc.* **1978**, *100*, 8264.